

Moving contact lines in heated liquid film ¹

Ana Oprisan², John Hegseth², Y. Garrabos³, and D. Beysens³

1 Paper presented at the Fourteenth Symposium on Thermophysical Properties, June 22-27, 2003, Boulder, Colorado, U.S.A.

2 Department of Physics, University of New Orleans, New Orleans, Louisiana 70148, U.S.A. To whom correspondence should be addressed.

3 ESEME, Institut de Chimie de la Matière Condensée de Bordeaux, CNRS, Université de Bordeaux I, Avenue du Dr. Schweitzer, F-33608 Pessac Cedex, France.

ABSTRACT

Using a defocused grid method, we studied the dynamics of a triple contact line in pure fluid near its critical temperature. A cell containing a gas bubble surrounded by liquid and squeezed between two sapphire plates produced a large region on the plates covered with a liquid film. The sapphire cell walls allow light to pass through the two thin wetting films of liquid surrounding the flattened gas bubble. The cell was heated in weightlessness on the Mir space station. This heating resulted in a film thickness change that was observed using a defocused grid method where liquid-gas interface curvature refracts parallel incident rays, displacing the shadows of a wire grid placed in front of a recording camera. During heating, a low-contrast line appears on the wetting film that corresponds to a sharp change of the wetting film thickness. We have analyzed this liquid-gas-sapphire contact line. We also discuss the possible causes of the movement of the contact line, especially the interfacial stress from gas condensation and evaporation induced by heating.

KEY WORDS: contact line, surface tension, evaporation, vapor recoil

1. Introduction

When two-phase fluid (single species fluid with coexisting gas and liquid) is heated past its boiling point, a complex process of fluid dynamics, interfacial phenomena, and heat transfer take place [1]. This process is greatly complicated by thermal convection. The buoyancy from gravity also lifts gas bubbles from a hot surface when it overcomes a competing force from surface tension that holds the bubbles on the hot surface. When the gas bubble grows sufficiently this buoyancy overcomes the surface tension and the bubble goes upward. In weightlessness, the buoyancy force is eliminated allowing this process to be observed under simplified conditions. Close to the critical region, many thermodynamics properties, including the surface tension, vary according to well-known universal power law [2], [3]. Near the critical point the fluid also exhibits perfect wetting of almost any solid. In a boiling process when the heating is applied in a two-phase fluid we can expect a perfectly wetted wall to dry from evaporation resulting in liquid-gas-solid triple contact lines.

We have made these simplifications in our experiments by using a simple pure fluid whose temperature is slightly below its critical temperature and whose density is nearly critical, so that the gas and liquid coexist. The experiments presented in this paper were performed in weightlessness on the MIR space station using the ALICE II instruments to suppress buoyancy driven flows and gravitational constraints on the liquid gas interface. Our thin constant volume cell, filled with SF_6 , produces a considerable constraint on the bubble and allows the entire bubble to be observed as heat is applied [4]. The initial response of the bubble to the temperature increase occurs at the edge of the bubble where the grid line becomes distorted. This distortion propagates into the

bubble and causes the change in the thickness of the wetting film. Assuming a triple contact line, we estimate the film thickness change that quantitatively follows a contact line spreading event.

The cylindrical cell, shown in Figure 1A, is 12 mm in diameter and 1.664 mm thick while each sapphire window is 9 mm thick. A 10 mm diameter ring was engraved on one of the sapphire windows of each cell in order to calibrate the size of the visible area of the cell image (Figure 1B). The sample cell was placed inside a copper housing, in turn, was placed inside a thermostat (not shown). Heat was pumped into and out of the sample cell unit using six Peltier elements. The temperature was sampled every second and is resolved to 1 μ K [5]. Although the cell was manufactured with high precision, the cell's windows could not be placed exactly parallel because the windows are pressed and glued in the copper housing leaving a glue layer. The influence of the windows' tilt angle on the position and shape of the gas bubble is discussed in [5]. The off-center position of the gas bubble (Figure 1B) is caused by the windows' tilt.

The explanation for the recorded image on the CCD plane is as follows [6]. A plane wave propagating in the x-direction illuminates a phase object (Ω) that is a single bubble in a thin constant mass cell filled with fluid near its critical density (Figure 1A). An image of Ω is projected onto a plane Π by a lens L. A grid made up of equally spaced straight wires (with periodicity p and thickness a) is placed perpendicular to the optical axis x , and parallel to the y -axis, between the L and Π [6]. The image of the grid is recorded in the plane Π by the sensitive array of a CCD video camera. The origin of the x -axis is taken as the entry-side of the cell Ω (point O). The distance between Ω and L is x_1 and the distance from L to Π is x_2 . Therefore, the magnification of the optical system

is given by $\gamma = x_2/x_1$. The distance of the grid to Π is x_g . If the gas-liquid interface is flat (see Figure 1A) then the incident rays, which are parallel with the optical axis Ox , would remain parallel with the optical axis after they cross the cell. The resultant image of the grid shadow is not distorted. The only indication of the cell presence is the dark gas-liquid interface because the meniscus refracts the normally incident light away from the cell's axis and out of the optical system.

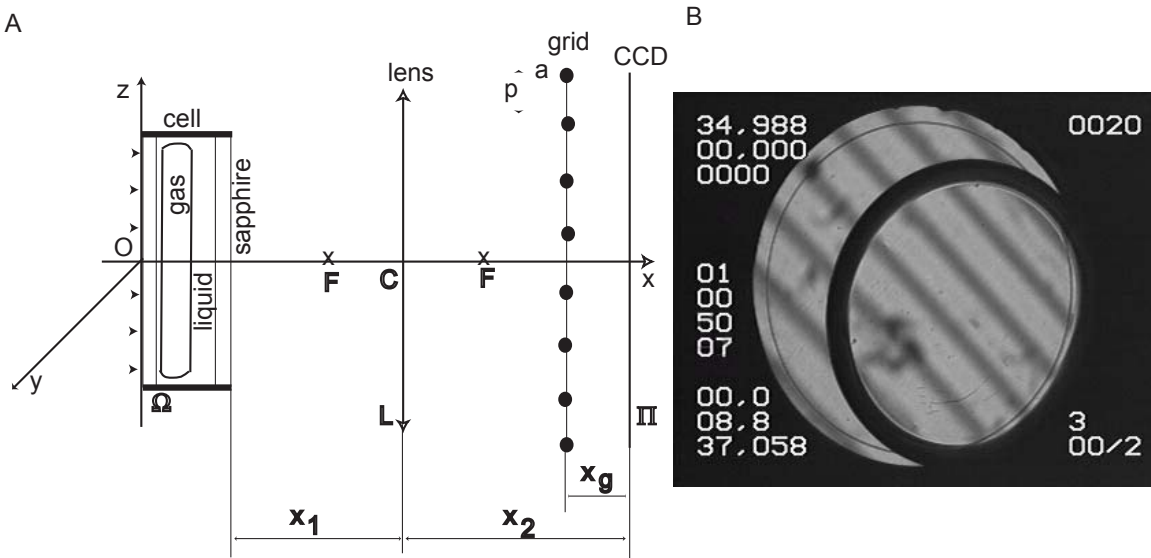


Figure 1. A) A schematic representation of the optical system and the cell. B) The corresponding image recorded by the CCD. The cell consists of a 12 mm diameter cylinder made of CuBeCo containing a 1.664 mm thin layer of SF_6 sandwiched between two sapphire windows (9 mm thick). The convergent lens, L, that has a focal point F and a center C, projects the out-of-focus grid image on the CCD plane Π (see panel B). The grid line shadow is not distorted indicating the existence of a flat gas-liquid interface.

During heating of the cell two phenomena take place. The first is the occurrence of a triple contact line (sapphire-gas-liquid) as shown in Figure 2A. Because the cooper conducts heat faster than sapphire the evaporation is stronger at the part of the interface

closer to the copper heating wall. The contact line spreads on the sapphire window(s), occurring on the thin liquid film in the bubble region. As explained in reference [4], the tilted sapphire window pushes the bubble to the side-wall leading to a contact between the bubble and the copper wall, i.e., there is a thin liquid layer between the gas bubble and the copper side-wall. Second, during the temperature increase toward T_c liquid evaporation leads to the gas bubble spreading phenomenon shown in Figure 2B where the contact angle shown in figure 2B appears to increase to $\approx 120^\circ$. The analysis of the gas-liquid interface demonstrates the existence of the differential recoil vapor force [7]. Besides the spreading that takes place at the copper wall, there is a similar process of liquid evaporation at the two sapphire windows. The evaporation of the thin fluid film between the sapphire windows and the gas bubble lead to the triple contact line (Figure 2A). Although the two processes are similar the major difference consists in a much higher heat transfer through the copper wall than through the sapphire window. As a result, we would expect the speed of contact line motion to be smaller than the change rate of the contact angle (Figure 1A).

2. The method

The principle of the measurement is the following. In the presence of any liquid-gas interface along the z-axis in the phase object (cell) Ω , the incident rays are deflected from their original direction. The deformation of the wave front causes a displacement and/or a distortion of the shadow of the grid on plane Π . The contact line in Figure 2a is typical of the dark localized lines that appear in this experiment. This dark line is caused by the curvature at the two edges of the contact line. The wetting condition of the

interface at the wall requires a concave curvature near the wall while the flat interface away from the contact line requires convex curvature. In between there is an inflection point and the entire variation of slope has a mean value. This suggests that between these edges of the contact line a linear approximation to the shape should be reasonable simplification that allows an estimate of the film thickness. Using this wedge model, the shadow displacement depends on the angle of the interface, as shown in Figure 3. The ray tracing program we wrote uses a large number N ($10^3 - 10^6$) of equally spaced incident rays. For each incident ray, the position of the point of incidence on the CCD plane is computed to get the out-of-focus image of the grid by ray tracing (Figure 1B).

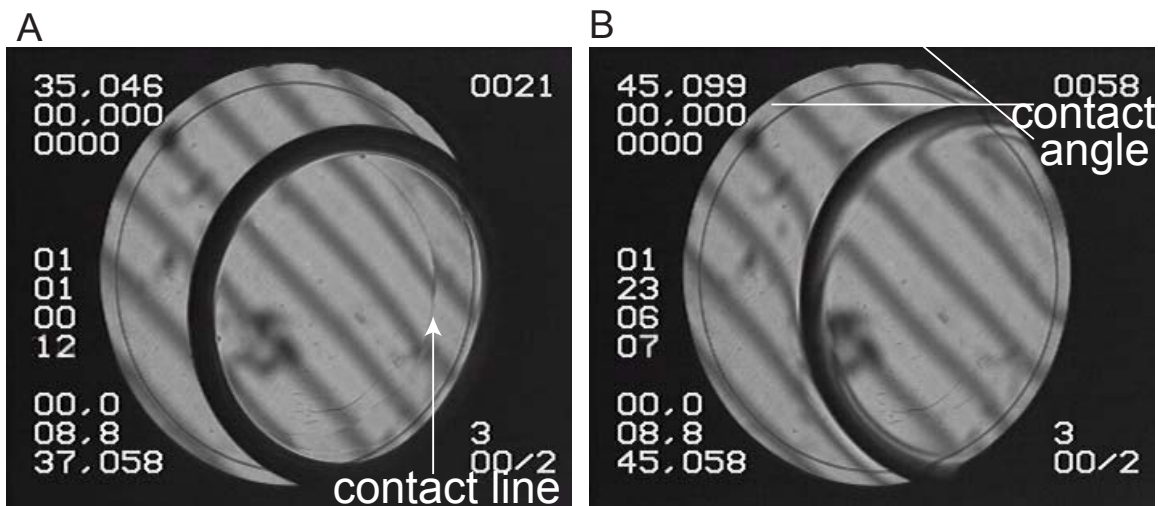


Figure 2. (A) The evaporation of the liquid film between the sapphire window(s) and the gas bubble leads to a triple contact line. (B) The heat transfer through the copper cell's side-wall leads to a rapid evaporation of the thin liquid film and a rapid change in the contact angle.

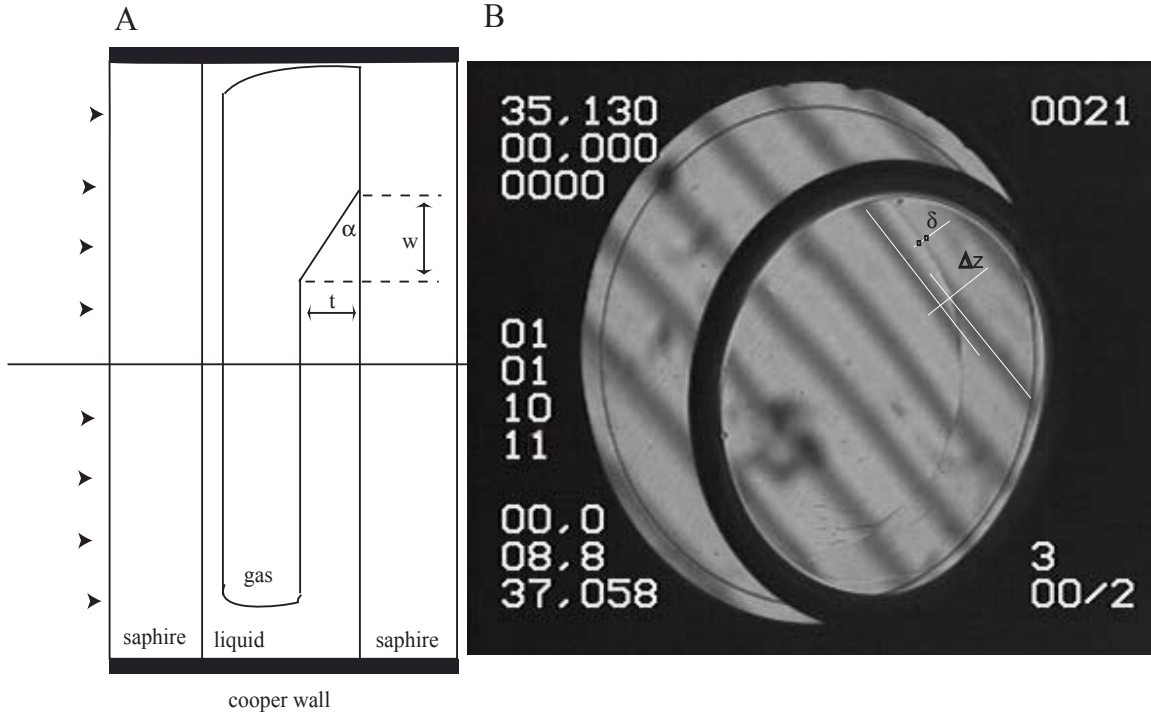


Figure 3. The tilted gas-liquid interface due to liquid evaporation leads to a triple contact line for gas-liquid-sapphire (panel A). The tilt angle induces a significant displacement of the grid shadow (panel B). The shadow displacement is proportional to the tilt angle (α) and the thickness (t) of the film.

If the gas-liquid interface is tilted ($\alpha \neq 0$), then it suffers successive refractions at the gas-liquid interface, liquid-sapphire interface, and, sapphire-air interface (see Figure 3) and the lens. The displacement of the grid shadow, $\Delta z(t, \alpha)$, depends on both the tilt angle (α) and the thickness of the gas-liquid interface (t).

$$\Delta z_6(t, \alpha) = - (t \tan(\alpha - r_1) + H_s \tan r_2) \gamma, \quad (1)$$

where r_1 is the refracted angles at the wedge, r_2 is the refracted angles at the liquid-sapphire interface, and H_s is the thickness of the sapphire window. From experimental data such as shown in Figure 4 we can measure $\Delta z(t, \alpha)$, and the width of the triple contact line in the image plane (δ). The width (w) of the tilted region can be obtained by using the

magnification formula $w = \delta/\gamma$, where γ is the optical system magnification. The width of the triple contact line is given by (Figure 3),

$$t = w \tan \alpha. \quad (2)$$

Using the relationship (2) we eliminate the tilt angle from (1) and numerically solve the equation for t . The tilted gas-liquid interface and its effect is shown in Figure 3.

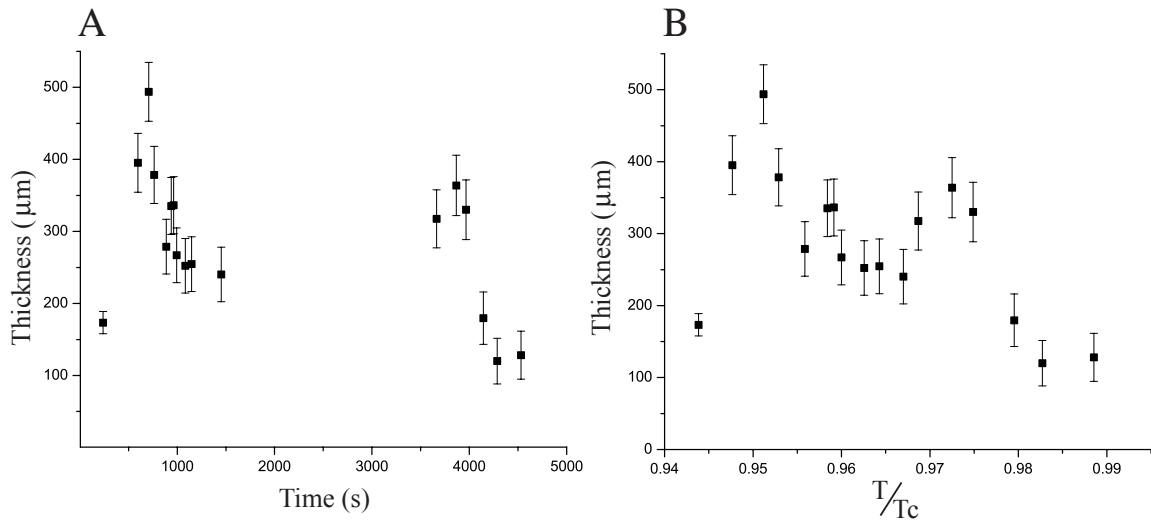


Figure 6. Estimated thickness of the film structure plotted versus time (panel A) and versus the relative temperature (panel B) for both temperature ramps. Data are for the second line above the black reference line drawn on Figure 5. The error bars reflect the uncertainty in the measurements of the triple contact line width.

The displacement of the shadow line, Δz , is significantly larger than the width of the contact line (δ) between the wetting film and the dry area. The width of the contact line (δ) is sometimes very small, close to the image resolution limit. As a result, we took 5 to 10 different perpendicular sections of the contact line and determined the average width. Using the average value of the width, we computed, from formulas (1) and (2) the

thickness of the film. An example of these measurements is shown in Figure 6 for two temperature ramps discussed below. The biggest error in thickness evaluation is from the uncertainty in the contact line width. Therefore, we computed the thickness of the film for the average width of the contact line and for the average width plus/minus its standard deviation the error bars in Figure 6.

3. Results and discussion

The temperature profile for this experiment consists of two ramps (10 mK/seconds) separated by a 40 minute constant temperature plateau. During this ramp the contact line often exhibits an apparent periodic change in position. The contact line on the B-H images often advances and retreats with a period of approximately 10-12 seconds corresponding to the heating cycle of the instrument.

Right at the beginning of each heating ramp the grid shadow is not distorted at all (also see Figure 1B), indicating a flat wetting film. After heating is started a fast moving line appears from the region where the bubble touches the side-wall. This line propagates to the left. The left side of the line shows grid shadow distortions while the right side appears flat. We can not directly detect if there is any liquid is present on the right side. If there were appreciable liquid after the propagation of such a large distortion (contact line) we would expect there to be significant interfacial distortions. This implies that there is at least a flat thin liquid film or a “precursor film” to the right of the contact line. The contact line, however, always moves away from the region where the bubble is in contact with copper side-wall. This is also the region with the largest heat flux (heat conductivity of copper is larger than that of sapphire) and this hotter region would tend to quickly evaporate any thin film to the right of the contact line. In addition, we have observed

similar moving lines in other cells where there are some particles deposited on the sapphire windows that act as a defect that clearly pins the contact line as it advances or retreats. Garrabos et. al. [4], [5] observed a striking spreading bubble event that occurs closer to T_c , and reasoned that a strong vapor recoil force, that diverges strongly at T_c , was pushing the bubble interface. As in that case, the vapor recoil (also called vapor thrust) is the only effect that we can find that could cause such a large mechanical force to push the contact line in these circumstances. In fact in this run the same bubble spreading is also seen in this run closer to T_c .

The vapor recoil force is large in the vicinity of a triple contact line [8]. This can be seen qualitatively by considering that the liquid-gas temperature is fixed by the saturated vapor pressure whereas the wall's temperature is larger. Near the triple contact line, a large temperature gradient forms, and the largest portion of mass transfer also takes place there. The region behind the triple contact line becomes dry because of evaporation. We therefore identify the line as a triple contact line and the area to the right of the contact line as the dry area.

After less than 30 seconds, the speed of the rapid moving contact line decreases almost to zero as shown in Figure 9. After continued heating of the cell for more than 15 minutes, a slow decrease in the dry area occurs until it stabilizes to an almost constant value (see Figure 9). We discuss below these two different regimes of the triple contact line movement.

Fast moving contact line

At the beginning of both temperature ramps (after the heating starts) and intermittently during the ramp, a fast moving contact line is seen. This triple contact line

slows as it advances toward the cell center (Figure 9). The initial fast motion is sometimes accompanied by a slight change in the contact angle shown in Figure 2B. We suspect that this change is also caused by vapor recoil. The heat conductivity for copper is larger than for sapphire; therefore the film should evaporate on the copper wall sooner than on the sapphire windows and this evaporation exerts stress on the bubble's meniscus at the copper side-wall. The rapid increase of the dry area surface behind the contact line is the result of the fast evaporation that takes place first at the copper wall.

A quantitative measure of the increasing dry area is the speed of the contact line. To determine this speed we draw a radius from the cell center perpendicular to the triple contact line. By measuring successive intersections of the triple contact line with the reference radius we are able to determine the velocity of the contact line along the chosen direction. The measurements in Figure 9 show that the triple contact line first moves rapidly for approximately 20 seconds and after almost 30 seconds stops. We linearly interpolate between the initial six time points (first 20 seconds) to find the average velocity of the fast moving contact line.

Interpreted in light of the vapor recoil mechanism we can see that the evaporation process is initially very fast. We can see, however, that once the gas makes significant contact with the cooler sapphire window the evaporation rate decreases and the speed of contact line decreases until a steady state regime is reached.

The wetting film thickness versus time and position (measured from the heating wall towards the center of the cell) is plotted in Figure 11. During the fast advance of the contact line, it appears that the forcing near the contact line pushes the fluid to the left where it accumulates.

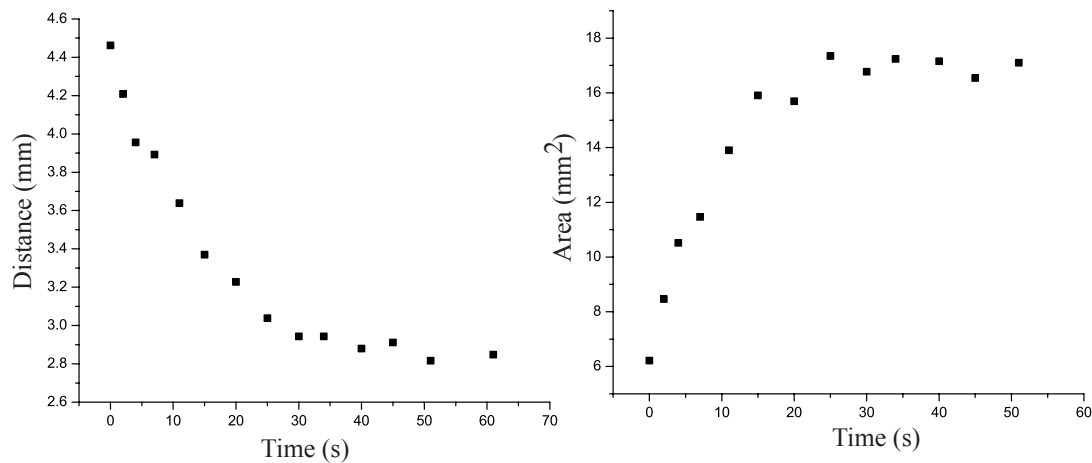


Figure 9. (A) Distance moved by the contact line towards the center of the cell after heating begins. (B) Consequently, the dry area left behind the triple contact line rapidly increases.

Slow dynamics of the contact line

We also studied the contact line over a longer time scale. After the initial fast motion the contact line (and the dry area behind) changes at a much slower rate. Measurements of the thickness of these slowly moving contact lines are shown in Figure 6. These measurements use the same linear model of the interface as used for the fast moving contact line. The errors shown in Figure 6 are derived from the errors in δ . We have also observed significant fluctuations in the film thickness in the slow regime.

At the beginning of each contact line advance, the dry area increases rapidly up to a maximum value, as discussed in the previous section. We plotted this maximum dry area over the longer time scale of the ramp as shown in Figure 12. We also note that the area of the bubble is essentially constant during the heating process (Figure 12 A and B). On the other hand, the relative surface dry area, as shown in Figure 12 C and D, has more complicated behavior. At first we observed a decrease in the dry area (Figure 12C and D)

but on a long time scale the surface of the dry area stabilizes to a constant value for a large range of the relative temperature (panel D).

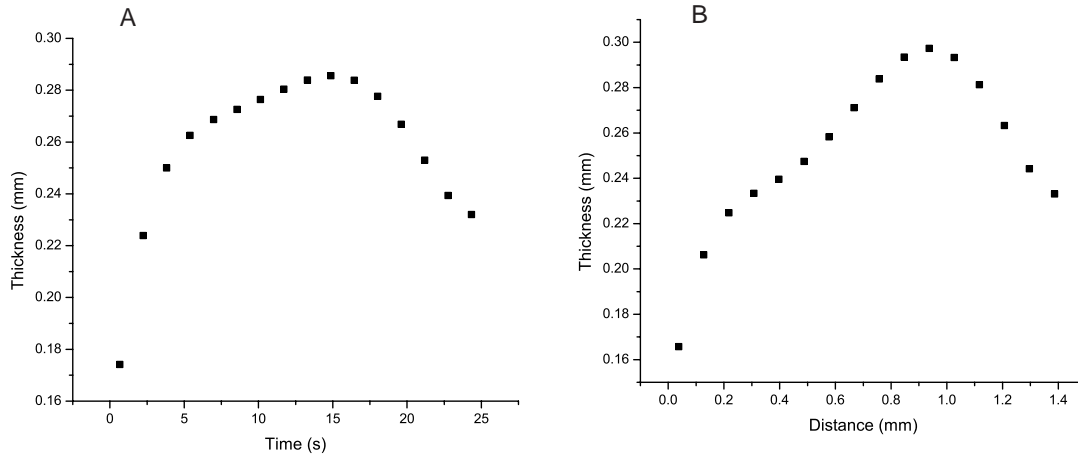


Figure 11. (A) Estimated thickness of the wetting film versus time measured from the beginning of the (second) heating ramp at the same position in the field of view. (B) Using the velocity of the contact line in Figure 9 we can estimate the spatial profile of the advancing contact line.

Figure 12 shows that the gas bubble area/volume stays constant while the dry area changes. There is also a strong correlation between the estimated film thickness in Figure 6 a with the total film surface area (Figure 12). This shows that the liquid film tends to conserve mass over the long time scale. At different temperatures a steady state is formed where the film thickness is small (large) and the dry area is small (large). The steady state is also accompanied by strong fluctuations in the film thickness after the initial fast advance. These fluctuations show that this steady state is a delicate balance between heat transfer, mass transfer, and mechanical stress.

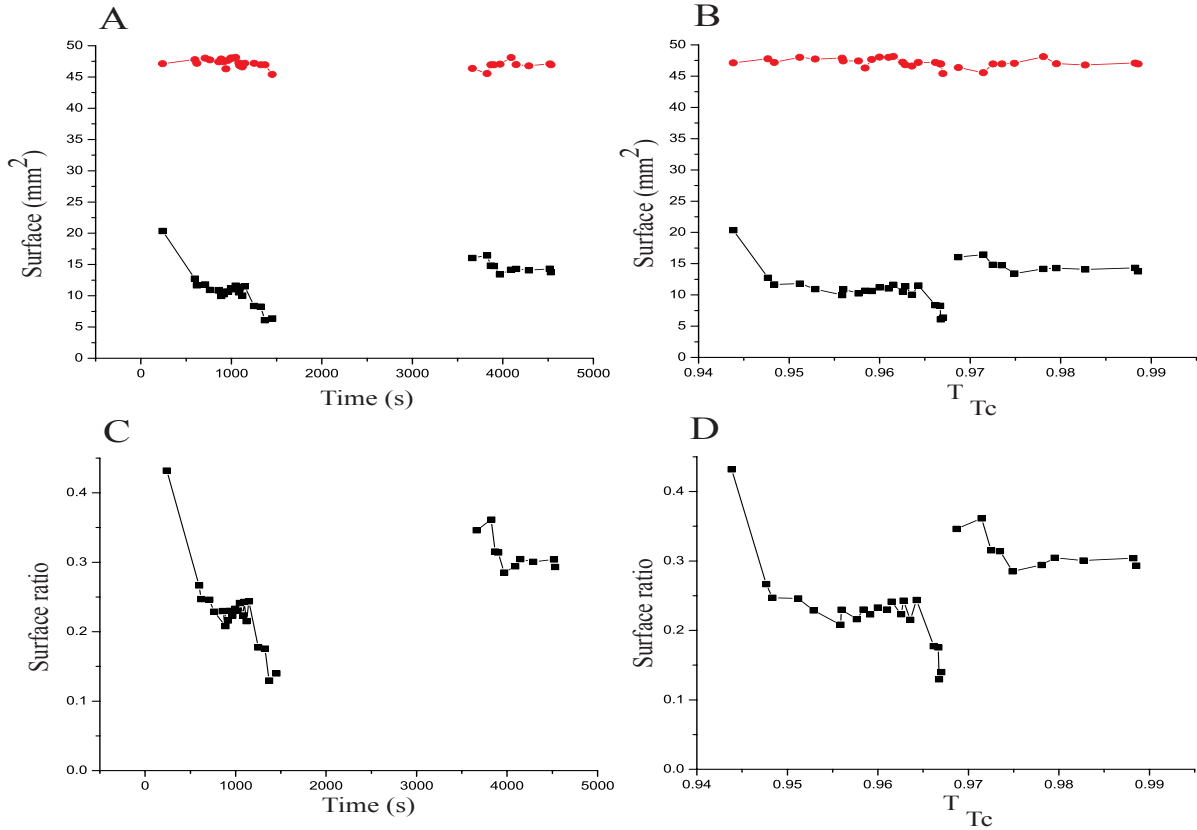


Figure 12 The total area covered by the dry area (black squares on panels A and B) and the area of the gas bubble (red data on panels A and B) versus time (panel A) and relative temperature (panel B). The total area of the gas bubble is constant during heating (red dots on panels A and B). The relative change in the area of the dry area versus time (panel C) and versus the relative temperature (panel D).

4. Conclusion

We used the grid-deflection method to estimate the thickness of the wetting film under microgravity conditions. We approximate the liquid-vapor interface near the contact line as a wedge, i.e., the contact line is an inclined plane between two parallel planes, where the incline is characterized only by its tilt angle with respect to the sapphire window. We have shown that the line observed in the 2D projection of the cell is a triple

contact line where the sapphire window has either a thin precursor film or has no film. The fast motion of the contact line appears to accumulate fluid in front of the line and the steady state line exhibits thickness fluctuations. We have been able to interpret our results using the vapor recoil force. The quantitative detail of the heat and mass transfer processes near the triple contact line is a challenging problem that exceeds the scope of this study. The qualitative explanation for the dynamics of the triple contact line is that the vapor recoil force exerts a stress on the vapor-liquid interface near the contact line.

ACKNOWLEDGEMENTS

We gratefully acknowledge the support of NASA through NASA-OBPS grants NAG3-1915 and NAG3-2447.

REFERENCES

1. L.S.Tong, “Boiling heat transfer and two phase flow”, (Taylor & Francis, New York, 1997).
2. . Green M.S. (ed.), “Critical Phenomena”, (Academic Press), 1971.
3. Moldover M.R., Sengers J.V., Gammon R.W., Hocken R.J., Rev. Mod. Phys., **51**, 79-99, 1979.
4. Hegseth J., Y. Garrabos, V. S. Nikolayev, C. Lecoutre-Chabot, R. Wunenburger, D. Beysens, International Journal of Thermophysics, **23**, 89 – 101, 2002.
5. Garrabos Y., Lecoutre-Chabot C., Hegseth J., Nikolayev V.S., Beysens D., Phys. Rev. E **64** (5), 051602-1 – 051602-10, 2001.
6. Gurfein V., Beysens D., Garraobs Y., and Le Neindre B., Optics Comm. **85**.
7. Palmer H.J., J. Fluid Mech., **75**, 487-511, 1976.
8. Nikolayev V.S., and D.Beysens, EuroPhysics Letters, **47**, (3), p.345 – 351, 1999.